Vascular Delivery of rAAVrh74.MCK.*GALGT2* to the Gastrocnemius Muscle of the Rhesus Macaque Stimulates the Expression of Dystrophin and Laminin α2 Surrogates

Louis G. Chicoine[1,3], Louise R. Rodino-Klapac[1,3], Guohong Shao[3], Rui Xu[3], William G. Bremer[4], Marybeth Camboni[3], Bethannie Golden[3], Chrystal L. Montgomery[3], Kimberly Shontz[3], Kristin N. Heller[3], Danielle A. Griffin[3], Sarah Lewis[3], Brian D. Coley[1,5], Christopher M. Walker[1,4], K. Reed Clark[1,3], Zarife Sahenk[1–3], Jerry R. Mendell[1–3] and Paul T. Martin[1,3]

[1]Department of Pediatrics, The Ohio State University and Nationwide Children's Hospital, Columbus, Ohio, USA; [2]Department of Neurology, The Ohio State University and Nationwide Children's Hospital, Columbus, Ohio, USA; [3]Centers for Gene Therapy, The Research Institute at Nationwide Children's Hospital, Columbus, Ohio, USA; [4]Vaccines and Immunity, The Research Institute at Nationwide Children's Hospital, Columbus, Ohio, USA; [5]Current address: Department of Radiology, University of Cincinnati College of Medicine, Cincinnati, Ohio, USA

Overexpression of GALGT2 in skeletal muscle can stimulate the glycosylation of α dystroglycan and the upregulation of normally synaptic dystroglycan-binding proteins, some of which are dystrophin and laminin α2 surrogates known to be therapeutic for several forms of muscular dystrophy. This article describes the vascular delivery of GALGT2 gene therapy in a large animal model, the rhesus macaque. Recombinant adeno-associated virus, rhesus serotype 74 (rAAVrh74), was used to deliver GALGT2 via the femoral artery to the gastrocnemius muscle using an isolated focal limb perfusion method. GALGT2 expression averaged 44 ± 4% of myofibers after treatment in macaques with low preexisting anti-rAAVrh74 serum antibodies, and expression was reduced to 9 ± 4% of myofibers in macaques with high preexisting rAAVrh74 immunity ($P < 0.001$; $n = 12$ per group). This was the case regardless of the addition of immunosuppressants, including prednisolone, tacrolimus, and mycophenolate mofetil. *GALGT2*-treated macaque muscles showed increased glycosylation of α dystroglycan and increased expression of dystrophin and laminin α2 surrogate proteins, including utrophin, plectin1, agrin, and laminin α5. These experiments demonstrate successful transduction of rhesus macaque muscle with rAAVrh74.MCK.GALGT2 after vascular delivery and induction of molecular changes thought to be therapeutic in several forms of muscular dystrophy.

Received 18 September 2013; accepted 12 October 2013; advance online publication 4 February 2014. doi:10.1038/mt.2013.246

INTRODUCTION

The *GALGT2* gene encodes a β1-4-N-acetyl-D-galactosamine (βGalNAc) glycosyltransferase that is known to glycosylate α dystroglycan in skeletal muscle.[1,2] GALGT2 adds a β1-4-linked GalNAc to Neu5Ac/Gcα2-3-Galβ1-4-GlcNAcβ-glycans to form Neu5Ac/Gcα2–3-[GalNAcβ1–4-]Galβ1-4-GlcNAcβ-, which is also called the cytotoxic T-cell (CT) glycan in mice and the Sd(a) blood group antigen in humans.[3] Muscle expression of GALGT2 and the CT glycan is high in the early postnatal period, where CT glycan expression is evident around the entire myofiber membrane, but GALGT2 and the CT glycan become confined to the neuromuscular junction in adulthood.[4] Overexpression of GALGT2 in skeletal muscle of adult mice stimulates the ectopic glycosylation of the extrasynaptic membrane with the CT glycan. This, in turn, induces the ectopic overexpression of normally synaptic dystroglycan-binding proteins, including utrophin, laminin α4, laminin α5, and agrin, as well as plectin1.[2,5,6] In addition to inducing the expression of proteins, GALGT2 glycosylation strengthens extracellular matrix binding to α dystroglycan and prevents eccentric contraction-induced muscle injury.[6,7] Gene transfer using the adeno-associated virus (AAV) vector rAAVrh74.MCK.GALGT2 also accomplishes prevention of muscle damage in the mdx mouse model for Duchenne muscular dystrophy (DMD),[7] the dy^{W} model for MDC1A[8] and the *Sgca*$^{-/-}$ mouse model for LGMD2D.[9] Other surrogate gene therapies that can ameliorate muscular dystrophy include utrophin,[10] integrin α7[11], and sarcospan[12] in dystrophin-deficient mice and laminin α1[13] and mini-agrin[14] in laminin α2-deficient mice.

To achieve maximal clinical benefit in muscular diseases, recombinant AAV (rAAV) likely will have to be administered via the vasculature. We have demonstrated that rAAVrh74 can deliver micro-dystrophin or *GALGT2* using an isolated focal

The first two authors contributed equally to this work.

Correspondence: *Louise R. Rodino-Klapac, The Research Institute at Nationwide Children's Hospital, 700 Children's Dr., Columbus, Ohio 43205, USA. E-mail: Louise.Rodino-Klapac@nationwidechildrens.org or Louis G. Chicoine, The Research Institute at Nationwide Children's Hospital, 700 Children's Dr., Columbus, Ohio 43205, USA. E-mail: Louis.Chicoine@nationwidechildrens.org or Paul T. Martin, The Research Institute at Nationwide Children's Hospital, 700 Children's Dr., Columbus, Ohio 43205, USA. E-mail: Paul.Martin@nationwidechildrens.org*

limb perfusion model via the femoral artery in the mdx mice[7,15] and that rAAVrh74 also efficiently induces muscle gene expression after intra-arterial administration in the rhesus macaque.[15] These findings are similar to studies utilizing rAAV8,[16] with which rAAVrh74 shares 93% sequence identity. Here, we have chosen the rhesus macaque for the first study of rAAVrh74.MCK.GALGT2 gene transfer in a large animal model, as macaques possess neutralizing antibodies to rAAVrh74 vector and a vascular limb anatomy that is similar to humans.[17,18]

RESULTS

Intramuscular delivery of rAAVrh74.MCK.GALGT2 in the rhesus macaque

We first treated one rAAVrh74 serum antibody-naive rhesus macaque by direct muscle injection to verify that we could assay for overexpression of the human GALGT2 gene, much as we had done previously in mice.[1,2,5,7–9] To do this, we injected the tibialis anterior (TA) muscle with 5×10^{12} vector genome (vg) rAAVrh74.MCK.GALGT2. The contralateral TA was mock-injected with an equivalent volume of sterile saline. The muscle was biopsied at 8 weeks after injection and frozen for immunostaining of cross-sections with the CT2 monoclonal antibody (**Figure 1**). In untreated muscle, CT2 expression was confined to blood vessels, capillaries, and neuromuscular junctions, as we had found previously in mice and humans.[4,19] By contrast, CT2 was overexpressed uniformly along the sarcolemmal membrane of skeletal myofibers in the rAAVrh74.MCK.GALGT2-treated muscle (**Figure 1**). GALGT2 expression assayed in this way approached 100% of all myofibers in muscle blocks harvested from the injected region. Thus, rAAVrh74.MCK.GALGT2 muscle transduction in the rhesus macaque could be easily visualized by assessing the end product of GALGT2 activity, the CT glycan.

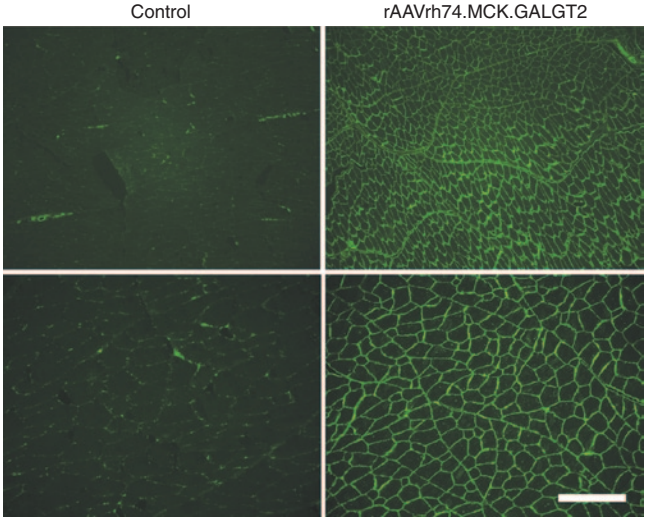

Figure 1 Expression of GALGT2 expression by cytotoxic T-cell (CT) carbohydrate immunostaining in rhesus macaque skeletal muscle. One tibialis anterior (TA) was injected with 5×10^{12} vg rAAVrh74.MCK.GALGT2, whereas the TA in the contralateral limb (control) was mock-injected with vehicle alone. After 8 weeks, a section of each muscle was stained with CT2 to determine transgene expression. Bar = 200 µm (lower panels) and 500 µm (upper panels). rAAVrh74, recombinant adeno-associated virus, rhesus serotype 74.

Vascular delivery of rAAVrh74.MCK.GALGT2 to muscle is dependent on rAAVrh74 serostatus

For vascular delivery, a fluoroscopically guided catheter was placed in the femoral artery at the apex of the femoral triangle and advanced into the sural artery. The sural artery feeds both the lateral and medial heads of the gastrocnemius. Two tourniquets, one placed just proximal to the catheter tip and the other placed distal to the gastrocnemius, compartmentalized the region for vector delivery. 2×10^{12} vg/kg of virus was delivered in a volume of 2.5 ml/kg normal saline and allowed to dwell in the isolated limb for 10 minutes, much as we have reported previously.[15] End point analysis was completed 12 or 24 weeks postvector administration, at which time both the treated and contralateral gastrocnemius muscles were removed and snap frozen. Biweekly analysis of serum and blood chemistries showed no sign of significant changes as the result of treatment from 2 to 22 weeks, relative to baseline values (**Supplementary Table S1**).

For analysis of GALGT2 expression, each head of the gastrocnemius was dissected into 15–18 blocks of tissue, each 23–35 mm^2, taken equally from the proximal, central, and distal muscle region. Every segment was subsequently cut into 1.45 mm^2 blocks, usually four per segment, and at least 1,200 myofibers per segment analyzed for CT2 staining, as described in Chicoine *et al.*[20] The percentage of myofibers in each segment expressing CT2 was reconstituted into a heat map to indicate the delivery of rAAVrh74.MCK.GALGT2 throughout the entire muscle (**Figure 2**). CT2 expression was high in most muscle segments for each treated muscle in macaques lacking preexisting serum antibodies to rAAVrh74 (serum-naive) at the time of treatment (**Figure 2**), while all contralateral stained as shown in **Figure 1**. The average expression was 45 ± 11% of myofibers for all treated serum-naive macaques (both 12 and 24 weeks posttreatment), as compared with 14 ± 6% of myofibers for similarly-treated macaques with preexisting rAAVrh74 antibodies ($P < 0.05$; analysis of variance; $n = 6$ per group, all without additional immunosuppression) (**Figure 3a**). Antibody-positive (preimmune) macaques were defined by an enzyme-linked immunosorbent assay (ELISA) optical density reading for rAAV-binding antibodies above 0.1 for a 1:800 dilution of serum. CT2 expression for the summed segments of each gastrocnemius muscle was as high as 74% at 24 weeks in antibody-naive macaques, whereas it never exceeded 13% for treated macaques with preexisting immunity. No necrosis and absent to mild mononuclear cell infiltration was present in all rAAVrh74.MCK.GALGT2-treated gastrocnemius muscles (**Figure 3b**). In addition, no significant difference in size of myofibers was observed between treated muscle and contralateral controls (**Figure 3c**). In addition, there was no significant alteration in percentage of type 1 versus type 2 fibers in treated versus untreated muscles (**Supplementary Figure S2**). The absence of muscle size or fiber type changes suggests a benign impact of GALGT2 overexpression on these parameters. Elevated rAAVrh74 serum antibodies were evident, both in naive and antibody-positive macaques, within 2 weeks after treatment (**Figure 3d**).

We utilized TaqMan quantitative polymerase chain reaction (qPCR) to quantify biodistribution of rAAVrh74.MCK.GALGT2 viral genomes in treated gastrocnemius muscle, contralateral (untreated) gastrocnemius muscle, popliteal lymph node (in treated gastroc), mesenteric lymph node, heart, lung, liver,

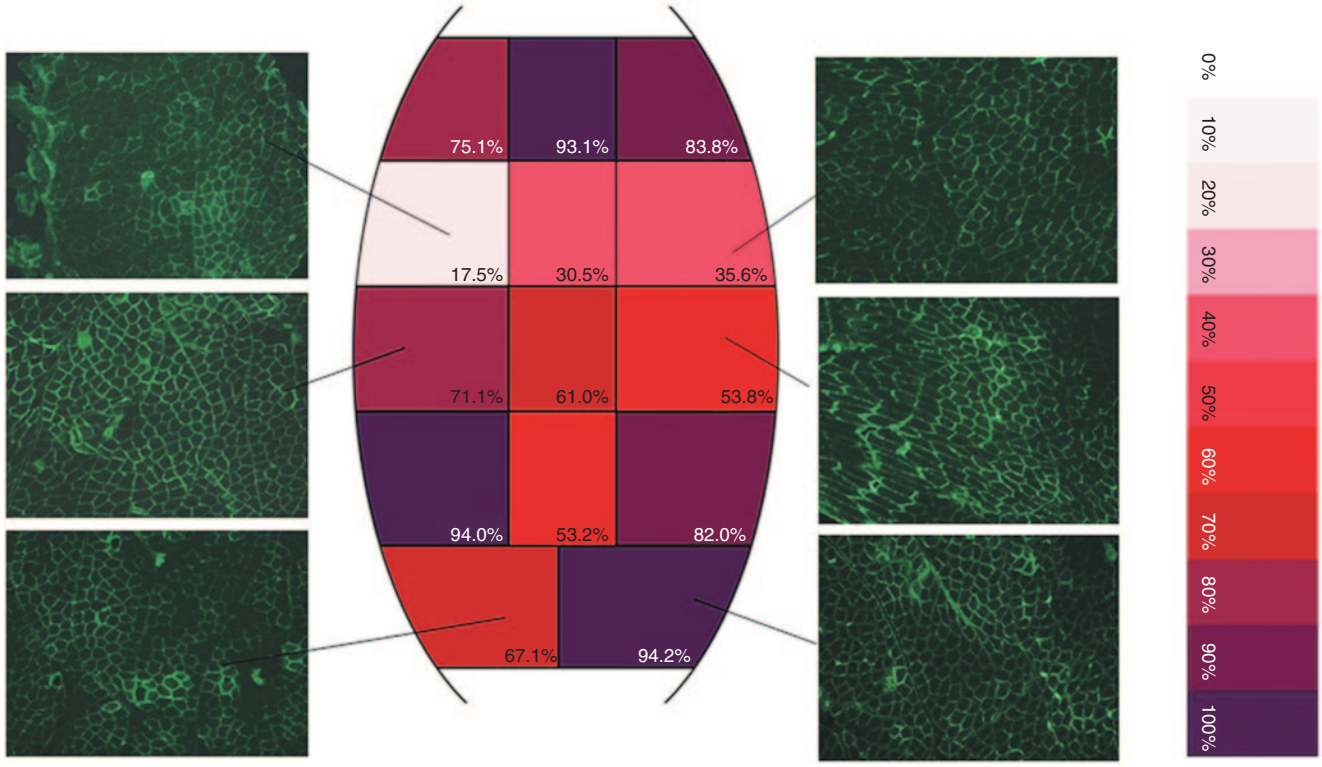

Figure 2 Heat map of cytotoxic T-cell (CT) glycan expression after isolated focal limb perfusion delivery of rAAVrh74.MCK.GALGT2 to the gastrocnemius muscle. The average percent muscle expression is shown for each block taken from lateral head of a gastrocnemius muscle treated with 2×10^{12} vg/kg rAAVrh74.MCK.GALGT2 12 weeks previously. Staining examples are from one of multiple sections imaged and used for quantification of each block. rAAVrh74, recombinant adeno-associated virus, rhesus serotype 74.

spleen, kidney, and gonad at 12 and 24 weeks after treatment (**Figure 4a**). Approximately 10^5 AAV vg/μg genomic DNA was present in the treated gastrocnemius muscle at 12 and 24 weeks, whereas less than 10^3 vg/μg was present in the contralateral control. Of the other tissues examined, the popliteal lymph node in the treated gastrocnemius showed the highest level of transduction (ca. 10^6 vg/μg). Liver and spleen also showed elevated transduction (ca. 10^5 vg/μg), whereas all other organs showed low levels of transduction (ca. 10^3 vg/μg). Of the six female and six male macaques analyzed, none showed detectable vector genomes (>50 vg/μg) in the gonads. We also analyzed GALGT2 messenger RNA expression in all of these organs by quantitative real-time PCR (qRT-PCR) (**Figure 4b**). As expected for the MCK promoter, only treated gastrocnemius muscles showed highly elevated GALGT2 transgene expression, ~100-fold relative to untreated muscle.

Role of immune suppression in rAAVrh74.MCK.GALGT2 therapy

We next compared eight different cohorts of three rhesus macaques each to address the role of immunosuppression. To do this, we compared treated macaques that were naive for antibodies to rAAVrh74 (antibody negative) at the time of treatment, macaques that had significant rAAVrh74 serum antibodies at the time of treatment, and macaques in the latter category that were additionally treated with one of the two immunosuppression regimens (prednisolone or triple therapy with prednisolone and the T-cell inhibitors tacrolimus, and mycophenolate mofetil (**Supplementary Figure S1**). Glucocorticoid therapy is the current standard of care in DMD, as it has been shown to prolong ambulation in patients.[21] While the glucocorticoid prednisolone is an effective immune suppressant, there is reason to believe that additional T-cell inhibition might be warranted in some muscular dystrophy patients treated with AAV vectors, as AAV treatment can induce additional T-cell responses to the capsid protein.[22] Therefore, we chose to add tacrolimus and myocophenylate mofetil to prednisolone as an additional condition, as these are T-cell inhibitors currently used in the clinical setting. Each immunosuppressive (IS) regimen was begun 2 weeks before rAAVrh74.MCK.GALGT2 treatment. While subtle, a comparison of pretreatment rAAVrh74 titers in the four IS cohorts with the four non-IS cohorts showed a modest (17%) reduction in Time 0 rAAVrh74 antibody titer for IS-treated animals. This change did not reach significance nor did the same comparison at 8 weeks post-GALGT2 treatment (serum titer 18 ± 4 IS versus 20 ± 8 non-IS, 1:800 ELISA). CT glycan expression in antibody-naive macaques averaged 56 ± 12% of myofibers at 12 weeks and 35 ± 30% at 24 weeks, whereas macaques with preexisting rAAVrh74 immunity at the time of treatment averaged 21 ± 20% of myofibers at 12 weeks and 9 ± 6% at 24 weeks (**Figure 5a**; $n = 3$ each). In rAAVrh74 antibody-positive macaques, the average serum ELISA reading was 5.5 (at 1:800 dilution), a 128-fold increase compared with serum-naive macaques, which averaged 0.043. Cohorts treated with prednisolone alone or with triple therapy did not significantly elevate CT glycan expression compared

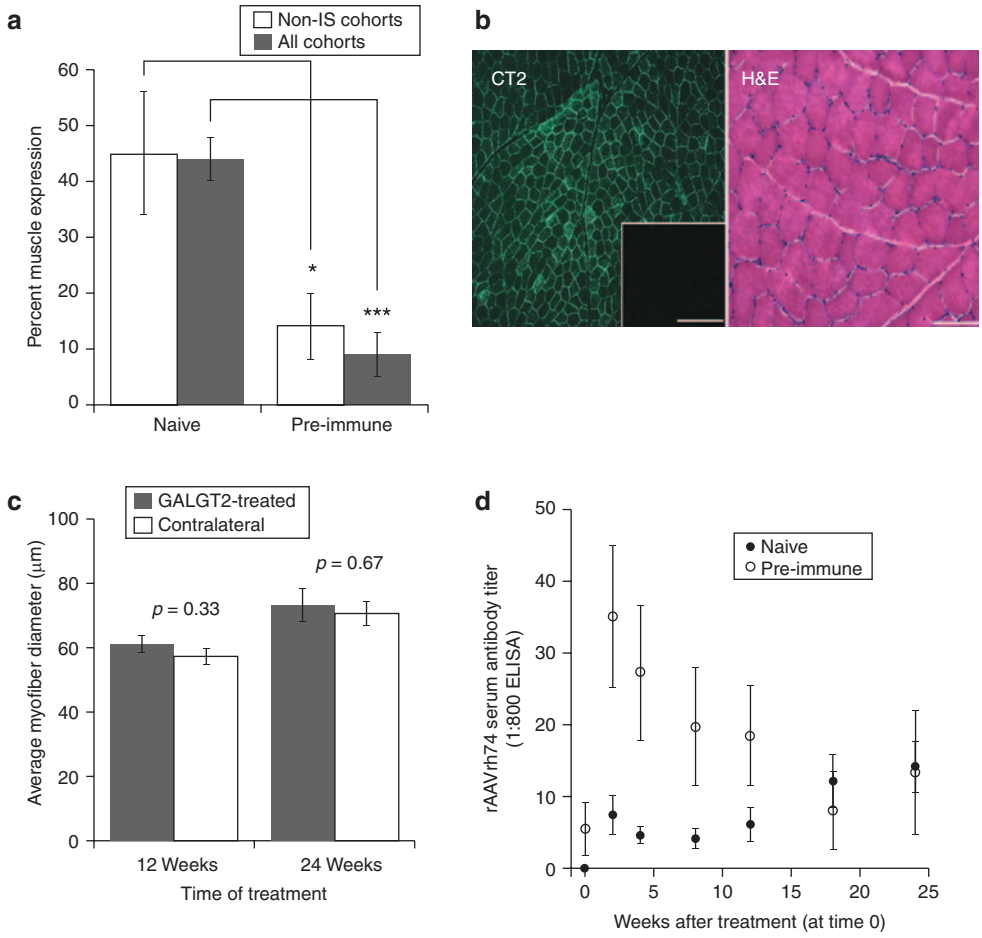

Figure 3 Effect of preexisting anti-rAAVrh74 immunity on muscle GALGT2 transgene expression. All macaques were treated with 2×10^{12} vg/kg rAAVrh74.MCK.GALGT2 via the isolated focal limb perfusion procedure. (**a**) The average of 12- and 24-week data from serum-naive macaques is compared with macaques with preexisting serum antibodies to rAAVrh74 (preimmune, defined as rAAV antibody enzyme-linked immunosorbent assay (ELISA) at 1:800>1.0). Open bars represent all animals not treated with immune suppression (non-IS). Errors for non-IS cohorts are SEM for $n = 6$ macaques per condition, $^*P < 0.05$. Dark bars represent all cohorts, including cohorts treated with immune suppression. Errors for all cohorts are SEM for $n = 12$ macaques per condition, $^{***}P < 0.001$. (**b**) Representative image of positive CT2 immunostaining in rAAVrh74.MCK.GALGT2-treated gastrocnemius muscles and of hematoxylin and eosin (H&E) staining. Inset in left panel shows staining with secondary antibody only. Bar is 200 μm (left panel) or 100 μm (right panel). (**c**) Average myofiber diameter (mini-Feret) between treated and contralateral untreated muscles was unchanged at 12 and at 24 weeks posttreatment. Errors are SD for $n = 3$ per condition. (**d**) rAAVrh74 antibody titers (1:800 dilution ELISA) in naive and preimmune macaques after treatment at time 0 with rAAVrh74.MCK.GALGT2. Errors are SD for $n = 3$ per condition. rAAVrh74, recombinant adeno-associated virus, rhesus serotype 74.

with serum-naive treated macaques, but CT glycan expression in these cohorts correlated with rAAVrh74 antibody titers at the time of treatment (Figure 5a,b). Overall, GALGT2 expression averaged 44 ± 4% of myofibers after treatment in macaques without high levels of preexisting anti-rAAVrh74 serum antibodies (defined as <1.0 at 1:800 ELISA), and expression was reduced to 9 ± 4% of myofibers in macaques with high levels of preexisting rAAVrh74 antibodies (defined as >1.0 at 1:800 ELISA; $P < 0.001$; $n = 12$ per group, pooled 12- and 24-week time points) (Figure 3a).

T-cell responses after rAAVrh74.MCK.GALGT2 treatment

We analyzed T-cell responses within peripheral blood mononuclear cells (PBMCs) using an interferon-γ enzyme-linked immunosorbent spot assay. We assayed responses to three overlapping peptide pools comprising the entire coding sequence of the rAAVrh74 capsid protein and two overlapping peptide pools comprising the entire coding sequence of the human GALGT2 protein (Figure 6a,b). T-cell responses (>50 spot-forming colonies (SFCs)/10^6 PBMCs) to rAAVrh74 capsid were rarely detected in the rAAVrh74.MCK.GALGT2-treated cohorts at 2–24 weeks posttreatment, though some modest responses in the 50–100 SFCs/10^6 PBMCs range were present in most posttreatment 2-week intervals, particularly for peptide pool 2 (Figure 6a). Two macaques (6–123 and 06C068) showed a late transient response to both GALGT2 peptide pools at 20 weeks after treatment (>200 SFCs/10^6 PBMCs; Figure 6b), with some elevated responses of >50 SFCs/10^6 PBMCs at other time points.

The two positive GALGT2 responses were mapped to a single GALGT2 peptide (peptide P5; Figure 6c). Further mapping of the epitope by N- and C-terminal truncation of the P5 peptide revealed that it is a nonamer spanning amino acids 89–97 of

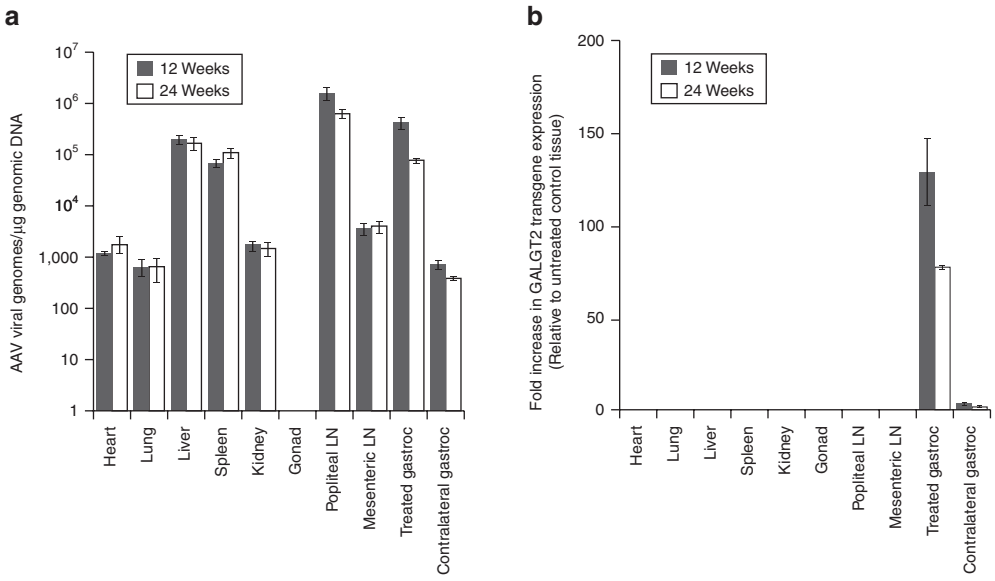

Figure 4 Recombinant adeno-associated virus (rAAV) biodistribution and *GALGT2* gene expression after vascular delivery of rAAVrh74.MCK.GALGT2. Serum-naive rhesus macaques were treated for 12 or 24 weeks with rAAVrh74.MCK.GALGT2. (**a**) Biodistribution of rAAV vector genomes (vg) was quantified in treated and control tissues per μg of genomic DNA. (**b**) GALGT2 transcripts arising from rAAVhr74.MCK.GALGT2 treatment were assayed by quantitative real-time-polymerase chain reaction. Errors are SEM for $n = 9$ measurements per condition in **a** and SD for $n = 3$ measurements per condition in **b**. LN, lymph node; rAAVrh74, rAAV, rhesus serotype 74.

GALGT2[23] (Figure 6d) and presented by the Mamu-A0201 class I molecule (not shown). Of the two amino acid differences between the human and rhesus P5 peptides, only the human methionine to rhesus threonine substitution fell within the minimal epitope at amino acid position 3 (Figure 6c,d). Substitution of this single human–rhesus difference within the P5 peptide (human methionine to rhesus threonine) was sufficient to eliminate T-cell recognition (Figure 6c). Thus, even though transient in nature, T-cell responses to the human GALGT2 occurred in several macaques after rAAVrh74.MCK.GALGT2 treatment, but such responses were specific for human–rhesus differences within the GALGT2 protein. The two macaques with a T-cell response to the human peptide showed mononuclear cell infiltrates in the treated muscle at 24 weeks (**Supplementary Figure S3**). These infiltrates contained $CD8^+$ T cells, with no appreciable CD14- or CD16-positive monocytes. Therefore, a T-cell response to the human GALGT2 protein in these two subjects (one from cohort 1 and one from cohort 3 (Figure 5a), both of which showed overall muscle expression of GALGT2 below 20%, could have impacted gene expression levels.

Induction of dystrophin and laminin α2 surrogates by rAAVrh74.MCK.GALGT2

Previous studies in mice have demonstrated that GALGT2 overexpression can induce the glycosylation of α dystroglycan with the CT glycan and induce the overexpression of normally synaptic dystroglycan-binding partners, including utrophin, plectin1, agrin, and laminin α5.[2,5,8,9] Some of these proteins are dystrophin or laminin α2 surrogates known to inhibit disease in mice models of DMD or MDC1A,[10,24] much as GALGT2 overexpression can.[2,8] Here, we analyze whether such changes can occur after vascular delivery of rAAVrh74.MCK.GALGT2 in rhesus macaque muscle (Figures 7 and 8).

To assess α dystroglycan glycosylation, nonionic detergent whole-cell muscle lysates were made from GALGT2-treated muscles at 12 and 24 weeks and from untreated controls. Each GALGT2-treated muscle had between 70 and 74% of myofibers expressing CT glycan, whereas less than 1% of myofibers expressed CT glycan in contralateral controls. We performed precipitations with a lectin that can bind the CT glycan (*Wisteria floribunda* agglutinin, WFA) and a control lectin that cannot (wheat germ agglutinin (WGA)) (Figure 7). At 12 and 24 weeks after treatment, WFA precipitated α dystroglycan in GALGT2-treated muscles even when low protein levels (0.15 mg) were used. By contrast, WFA precipitated α dystroglycan only when large amounts of cell lysates were used (1 or 3 mg protein) in contralateral control muscles. As in mice,[1] CT2 immunoblots of WFA precipitates showed positive signal at the molecular weight for α dystroglycan (160 kDa), with only several additional minor bands being present (**Supplementary Figure S6**). We determined that 18 ± 4% of total α dystroglycan was precipitated by WFA (relative to WFA + WGA) in control muscles. This increased to 57 ± 3% in 12-week treated and 71 ± 5% in 24-week treated muscles ($P < 0.01$ for both versus control; $n = 4$ each). As before,[1,2,5,6,8,9] both α and β dystroglycan coprecipitated in all experiments (Figure 7). Uncleaved 160–200 kDa αβ dystroglycan was also identified in immunoblots when high amounts of β dystroglycan were precipitated (**Supplementary Figure S7**), a species previously reported in some human tissues.[25] WGA precipitations yielded roughly equivalent amounts of α and β dystroglycan in all control and treated muscles. Dystroglycan immunoblots were stripped and reprobed for dystrophin or utrophin. As in muscles of mice,[26] WFA and WGA coprecipitated both utrophin and dystrophin along with dystroglycan in GALGT2-treated macaque muscles, with utrophin being particularly evident at 24 weeks after treatment.

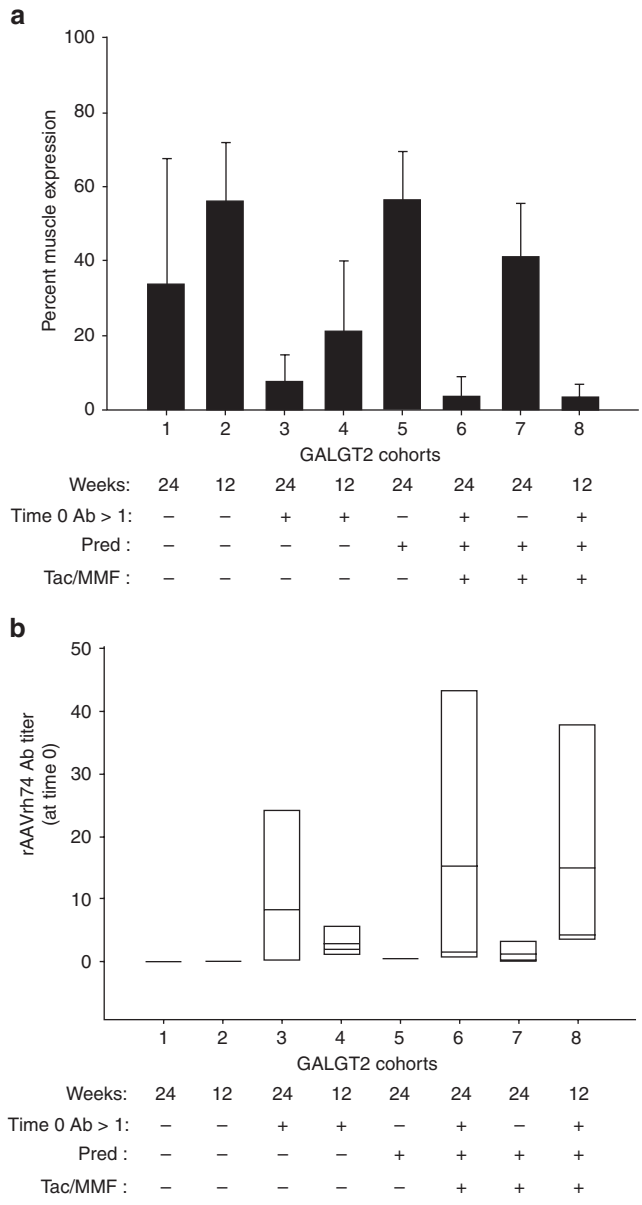

Figure 5 Effect of immune suppression on muscle GALGT2 transgene expression. Rhesus macaques were treated with 2×10^{12} vg/kg rAAVrh74.MCK.GALGT2 via isolated focal limb perfusion. (**a**) Summary graph of percentage of muscle fibers overexpressing GALGT2 in cohorts (of three macaques each) with low (Time 0 antibody (Ab) not >1 for serum enzyme-linked immunosorbent assay at 1:800 dilution) or high (Time 0 Ab>1 using the same assay) levels of preexisting rAAVrh74 serum antibodies in the presence and absence of immune suppression with prednisolone (Pred) or Pred with tacrolimus (Tac) and mycophenolate mofetil (MMF). Errors are SD for $n = 3$ animals per condition. (**b**) Summary box graph of serum rAAVrh74 antibody levels for each cohort represented in (**a**) measured on the day of vector administration, before treatment. The gray line represents the cohort mean and the box ends represent the 5 and 95% confidence intervals for the cohort. rAAVrh74, recombinant adeno-associated virus, rhesus serotype 74.

We next assessed whether rAAVrh74.MCK.GALGT2 treatment would cause overexpression of dystrophin and laminin α2 surrogates, as it is known to do in mice. To do this, we analyzed whole-cell protein expression by immunoblotting (**Figure 8a** and **Supplementary Figure S4**), messenger RNA expression by qRT-PCR (**Figure 8b**), and protein distribution by immunostaining (**Figure 8c** and **Supplementary Figure S5**). GALGT2 protein was overexpressed in all treated macaque muscles, while it was nearly undetectable in contralateral untreated controls, consistent with its normal confinement to the neuromuscular junction[1,19] (**Figure 8a**). There were significant increases in total protein expression for utrophin and plectin1, two potential dystrophin surrogates,[10,27,28] at 12 and 24 weeks after treatment (**Figure 8a** and **Supplementary Figure S4**). Utrophin protein levels were increased 2.2 ± 0.2-fold at 12 weeks and 3.5 ± 0.2-fold at 24 weeks, whereas plectin1 protein levels were increased 1.6 ± 0.1-fold at 12 weeks and 1.7 ± 0.1-fold at 24 weeks ($P < 0.001$ for all). Increased expression of utrophin was confirmed using two different monoclonal antibodies, one that recognizes the N-terminus (DRP2) and one that recognizes the C-terminus (DRP1) of the protein. Agrin and laminin α5, two potential laminin α2 surrogates, also showed significantly increased protein levels in GALGT2-treated muscles (agrin, 1.5 ± 0.1-fold and laminin α5, 2.0 ± 0.3-fold, both $P < 0.001$ versus contralateral control at 24 weeks; **Figure 8a** and **Supplementary Figure S4**). Immunoblots for normally extrasynaptic proteins, including dystrophin, α dystroglycan, β dystroglycan, and laminin α2, were largely unchanged in GALGT2-treated muscles, though some increases were evident. Immunoblots using an antiserum to the C-terminus of laminin α2 showed bands the native weight for the protein (ca. 350 kDa) and more prominent cleaved G domain fragment of 80–90 kDa, as occurs naturally in skeletal muscle.[29]

We next assessed whether increased protein levels were due, in part, to induction of transcription (**Figure 8b**). Transcription of GALGT2 was induced 82 ± 12-fold at 12 weeks and 112 ± 16-fold at 24 weeks in GALGT2-treated muscles ($P < 0.001$ for both versus untreated control). These results are consistent with the levels of gene overexpression from previous AAV-GALGT2 studies in mice.[8,9] Utrophin, agrin, laminin α2, and laminin α5 transcripts were significantly increased in GALGT2-treated muscles, again by as much as seen in previous mouse studies,[6] whereas dystroglycan, dystrophin, and plectin1 transcripts were unchanged (**Figure 8b**). Immunostaining for utrophin and laminin α5 showed high expression along the sarcolemmal membrane at 12- and 24-week post-treatment, while expression of both proteins was confined to intramuscular capillaries and neuromuscular junctions in untreated controls (**Figure 8c**). Neuromuscular junctions were visualized and confirmed by costaining with rhodamine-α-bungarotoxin, a probe that binds to nicotinic acetylcholine receptors concentrated in the postsynaptic muscle membrane (not shown). Staining for dystrophin, laminin α2, and β dystroglycan (**Supplementary Figure S5**) and staining for α dystroglycan, α, β, γ, and δ sarcoglycan (not shown) showed no change in GALGT2-treated muscles. Antibodies to agrin and plectin1 used for immunoblotting did not work for immunostaining. These data demonstrate that several normally synaptic dystroglycan-binding proteins, utrophin and laminin α5, had increased extrasynaptic distribution along the sarcolemmal membrane after rAAVrh74.MCK.GALGT2 treatment.

DISCUSSION

GALGT2 is a surrogate gene therapy that induces the ectopic expression of a complex of muscle proteins that, as a group, strengthen the muscle's resistance to injury and can inhibit

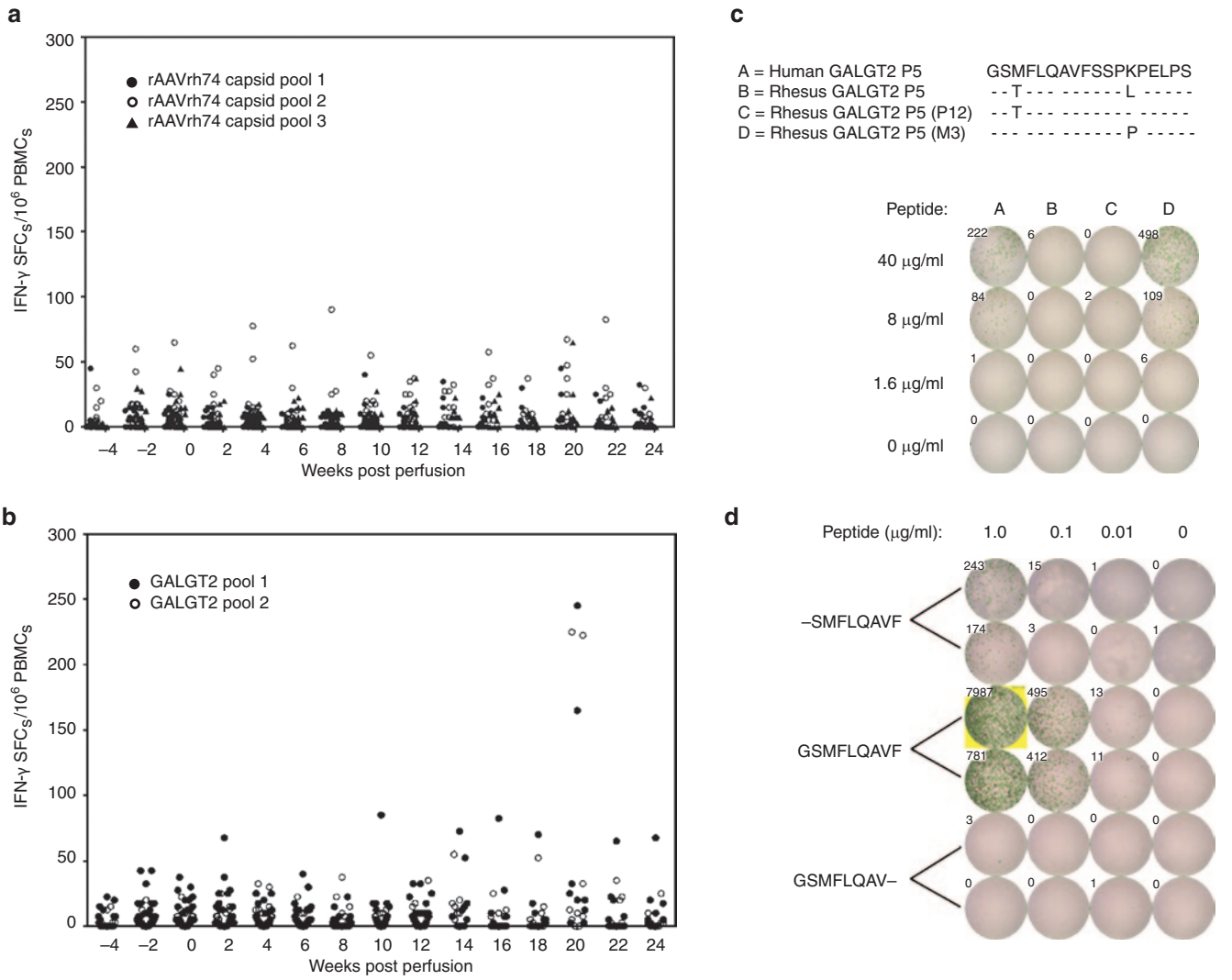

Figure 6 Enzyme-linked immunosorbent spot (ELISpot) assay for detection of rAAVrh74 capsid- or GALGT2-specific T cells in peripheral blood mononuclear cells (PBMCs). (**a**) Peptides comprising the entire AAVrh74 capsid protein were separated into three pools. There were mild transient responses to peptide pools in a few macaques that exceeded 50 spot-forming colonies (SFCs)/10^6 PBMCs. (**b**) Peptides comprising the entire GALGT2 protein were separated into two pools. There were significant responses in two macaques to GALGT2 peptide pools, particularly at 20 weeks. (**c**) Comparison of two ELISpot-positive GALGT2 pools identified a single responsive peptide with two human–rhesus amino acid differences, one of which, threonine (rhesus) to methionine (human), was necessary for positive response to the human P5 GALGT2 peptide. (**d**) ELISpot analysis of GALGT2 peptides maps the optimal N- and C-terminal ends for presentation of the ELISpot-responsive P5 peptide as glycine and phenylalanine, respectively. IFN-γ, interferon-γ; rAAVrh74, recombinant adeno-associated virus, rhesus serotype 74.

muscular dystrophy.[2,5,7–9] The advantages of using GALGT2 therapy, as compared with gene replacement, are its potential to treat more than one genetic form of muscular dystrophy and the likelihood of immune tolerance to the transgenic protein, which is endogenously expressed. Another potential advantage is that GALGT2 overexpression, in some cases, yields muscle protection that exceeds gene replacement, protecting even wild-type muscles from injury.[7] Previous studies in mice suggest that GALGT2 overexpression can be therapeutic in at least three forms of muscular dystrophy (DMD, MDC1A, and LGMD2D).[2,5,7–9] Despite the obvious advantages of testing gene therapies in mice, certain considerations relevant to treatment of human disease require validation in larger animal models that better approximate gene delivery in humans. Such considerations include dose confirmation, the scalability of rAAV production and delivery, and vascular, anatomical, and immunological interspecies differences. The vector dose we have used here to treat the gastrocnemius, 2×10^{12} vg/kg, is large, mirroring the high dose used in previous human clinical trials.[30,31] To treat entire limbs, additional technical advances, such as limb reperfusion, will likely be needed to lower the effective dose used in the clinic. Each of these issues represents a significant impediment to understand the full translational potential of any gene therapy treatment for muscle diseases. The present study is the first to demonstrate the ability to utilize vascular limb perfusion to treat a large animal muscle with GALGT2. While use of the rhesus macaque has advantages regarding modeling of immune responses to the rAAVrh74, a serotype isolated from macaques, rhesus macaques do not have muscular dystrophy. Treatment of a large animal model with muscular dystrophy, such as the GRMD dog,[32] will be required to further understand the translational

potential of rAAVrh74.MCK.GALGT2 in large animals. Those studies are currently ongoing.

We have demonstrated a strong correlation between GALGT2 expression and circulating antibodies to rAAVrh74, a serotype that appears to naturally infect rhesus macaques. This is in keeping with previous studies in mice,[33] primates,[34] and humans[30] that show the dramatic potential of neutralizing anti-rAAV antibodies to block tissue transduction. Of particular interest in considering therapeutic options was our attempt to modify preexisting immunity to enhance gene expression using pharmacologic treatment. Two approaches were used: prednisolone alone or an aggressive regimen consisting of triple therapy (prednisolone, tacrolimus, and mycophenolate mofetil). Neither approach significantly affected GALGT2 expression. Rather, the presence of anti-rAAV binding antibodies at the time of treatment was the primary effector of gene expression, regardless of immunosuppression. Our laboratory members[20] and others[35] have studied plasmapheresis as a means to lower preexisting rAAV antibody titer before rAAV treatment. Some such strategy will be needed to retreat patients with rAAV. Use of B-cell inhibitors has also been shown to accomplish this end.[36,37] A tangential issue, but one with potential relevance, is T-cell immunity to GALGT2 protein. Unlike gene replacement paradigms for muscular dystrophy, where patients, for example with DMD, may be immunologically prone to develop T-cell responses to the untolerized dystrophin protein,[38] surrogate gene therapies such as GALGT2 should be less impacted, as GALGT2 is expressed by almost all humans.[39–41] Indeed, the transient T-cell responses to GALGT2 that were identified were only due to a peptide where human–rhesus sequence differences were recognized, which should not occur in most human hosts. We cannot explain why this T-cell response occurred over such a short period of time and peaked so late after treatment (at 20 weeks), but this nevertheless may have impacted gene expression in the two animals where such T-cell responses occurred.

We have been able to show that GALGT2 overexpression in macaque skeletal muscle can stimulate the glycosylation of α dystroglycan and induce the ectopic overexpression of dystrophin and laminin α2 surrogates, including utrophin, plectin1, agrin, and laminin α5, much as previously observed in mice.[2,5,8,9] Glycosylation of α dystroglycan with the CT glycan by GALGT2 in mice can stimulate increased binding of muscle extracellular matrix proteins, including laminin α2, laminin α4, laminin α5, and agrin,[6] to α dystroglycan, which may strengthen dystrophin- and utrophin-associated glycoprotein complexes in the muscle membrane. Indeed, utrophin and dystrophin coprecipitated with dystroglycan in GALGT2-treated muscles, and utrophin protein levels were induced 3.5-fold by 24 weeks of GALGT2 treatment, an induction level suggested by Davies and colleagues as being sufficient to have therapeutic effect.[42] Notably, as in mice,[6] we also measured an increase in utrophin transcription after GALGT2 treatment. Therefore, GALGT2 overexpression may impact utrophin transcription and protein levels.

Like the CT glycan and GALGT2, most of the proteins overexpressed in GALGT2-treated muscles are normally expressed at high levels in skeletal myofibers after birth but become confined to the neuromuscular junction before adulthood.[3,4] The induction of these proteins by GALGT2, then, suggests the induction of a maintained juvenile muscle expression pattern that allows for the maintained overexpression of dystrophin and laminin α2 surrogates. While this may raise unforseen long-term safety issues for the muscle, for example, generation of auto-antibodies to GALGT2 protein, as is known to occur with the overexpression of other endogenous transgenic proteins,[43,44] our experimental data refute this scenario. GALGT2 transgenic mice, even with 1,000-fold levels of transgene overexpression in skeletal muscles, live a normal life span with no obvious untoward effects.[5] Moreover, GALGT2 and CT glycan levels are normally elevated in dystrophin-deficient mdx muscles[2,45] and show high expression in several adult human

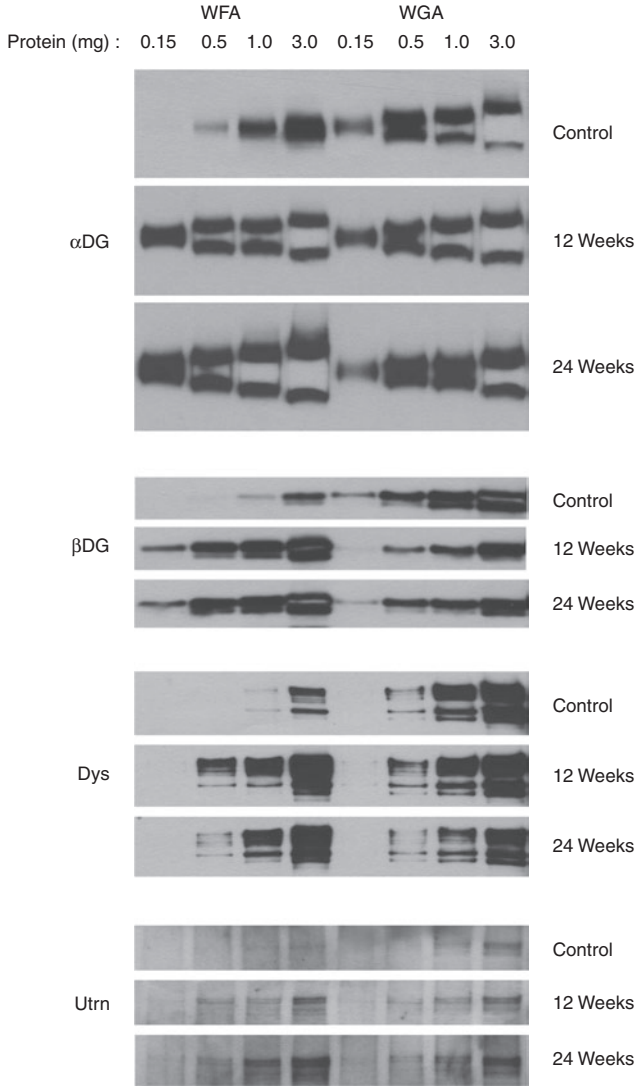

Figure 7 Glycosylation of α dystroglycan after rAAVrh74.MCK.GALGT2 treatment. Different amounts of NP-40 whole-cell lysates from GALGT2-treated and untreated muscles were subjected to precipitation by *Wisteria floribunda* agglutinin (WFA), a βGalNAc binding lectin known to precipitate α dystroglycan after glycosylation by GALGT2, or wheat germ agglutinin (WGA), a control lectin that precipitates α dystroglycan in the absence of GALGT2 activity. Proteins were separated on 4–12% gradient gels and subjected to Western blot using antibodies to α dystroglycan (αDG), β dystroglycan (βDG), dystrophin (Dys), or utrophin (Utrn). Molecular weights shown are 160 kDa for α dystroglycan, 43 kDa for β dystroglycan, and 400–430 kDa for utrophin and dystrophin. rAAVrh74, recombinant adeno-associated virus, rhesus serotype 74.

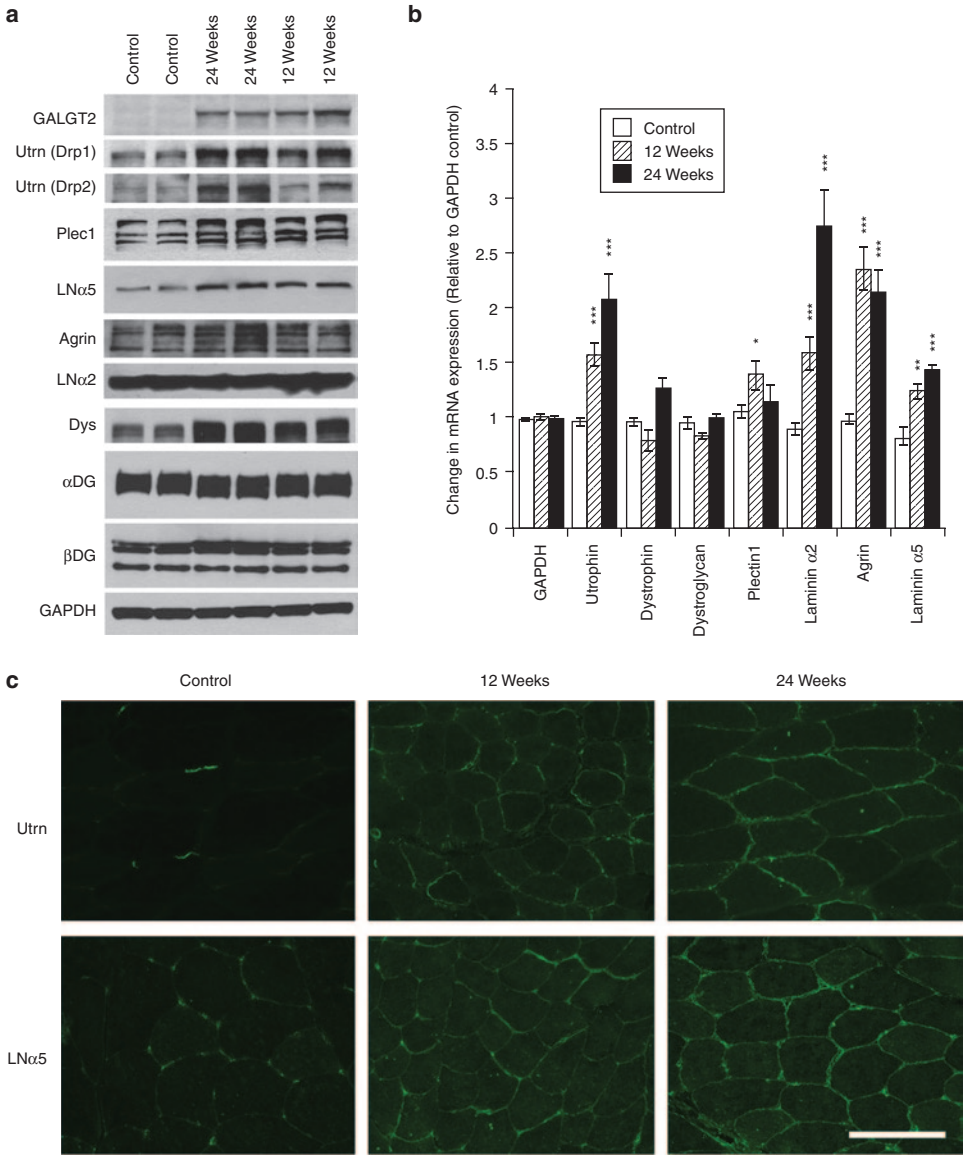

Figure 8 Upregulation of dystrophin and laminin α2 surrogate proteins in rhesus macaque muscle after GALGT2 overexpression. Serum-naive rhesus macaques were treated with 2×10^{12} vg/kg rAAVrh74.MCK.GALGT2 via the isolated focal limb perfusion procedure for 12 or 24 weeks and compared with untreated age-matched controls. (**a**) Western blots of protein expression on 20 µg of protein lysate were done using antibodies to GALGT2 (70 kDa), utrophin (400 kDa), plectin1 (300–600 kDa), laminin α5 (350 kDa), agrin (200–400 kDa), laminin α2 (80–90 kDa, principal band with C-terminal antibody), dystrophin(430 kDa), α dystroglycan(160 kDa), β dystroglycan (43 kDa, 30 kDa), and GAPDH (38 kDa). (**b**) Semi-quantitative real-time PCR was performed on messenger RNA purified from treated and untreated muscles to measure relative expression of rhesus utrophin, dystrophin, dystroglycan, plectin1, laminin α2, agrin, or laminin α5. Rhesus GAPDH was used as an internal control. Errors are SEM for $n = 6$–18 measurements per condition $^*P < 0.05$, $^{**}P < 0.01$, $^{***}P < 0.001$. (**c**) Utrophin immunostaining shows upregulation of utrophin protein along the sarcolemmal membrane in GALGT2-treated muscles. Staining for laminin α5 similarly showed upregulation in extrasynaptic regions of the basal lamina. Bar = 100 µm. rAAVrh74, recombinant adeno-associated virus, rhesus serotype 74.

tissues, particularly in the gastrointestinal mucosa.[39] Nevertheless, we cannot yet rule out that GALGT2 glycosylation of a certain protein or GALGT2-induced overexpression of certain proteins would have negative long-term consequences in humans, as animal models sometimes fail to predict human responses to rAAV treatment.[22] In GALGT2-treated macaques, however, we saw no change in muscle size, fiber type, or in serum enzyme markers for kidney, liver, or muscle function that would suggest induction of unwanted side effects, even with 100-fold levels of GALGT2 overexpression. While a number of issues related to innate and adaptive immune responses to AAV gene therapy treatments remain to be resolved,[31] the experiments presented here add to the profile of safety data demonstrating that vascular delivery of rAAVrh74.MCK.GALGT2 can induce GALGT2 overexpression accompanied by molecular changes with applications to several forms of muscular dystrophy.

MATERIALS AND METHODS

Macaques. All procedures were approved by the Research Institute at Nationwide Children's Hospital Institutional Animal Care and Use Committee.

Anti-rAAVrh74 antibody titer. These methods are identical to those described in ref. 20.

Vector production. rAAVrh74.MCK.GALGT2 was produced by a modified cross-packaging approach using AAV2 ITRs,[46] as described in ref. 20. A qPCR-based titration method was used to determine an encapsidated vector genome titer utilizing a Prism 7500 TaqMan detector system (PE Applied Biosystems, (Life Technologies), Grand Island, NY).[47] The primer and fluorescent probe targeted the MCK promoter and were as follows: MCK forward primer, 5-CCCGAGATGCCTGGTTATAATT-3; MCK reverse primer, 5-GCTCAGGCA CAGGTGTTG -3; and MCK probe, 5- FAM-CCAGACATGTGGCTGCTCCCCC -TAMRA-3.

Intramuscular injection. A rhesus macaque was anesthetized using Telazol (5 mg/kg intramuscularly) and treated with preoperative intramuscular Buprenorphine (0.01 mg/kg). The TA of both hindlimbs were shaved and prepared with 95% EtOH and Povidine solution, and the animal was secured to a warming blanket (37 °C) that overlies the surgery table. The TA was visualized by blunt dissection, and 5×10^{12} vg of rAAVrh74.MCK.GALGT2 or normal saline (1 ml volume total) was injected in three sites 0.5 cm apart. The fascial layer and skin incision was closed with 3–4 interrupted vicryl sutures and skin bond, and the injection site was marked with tattoo ink. For the muscle biopsy at 8 weeks, an incision was made to visually expose the TA muscle, using sterile drapes and scalpels. A small muscle biopsy was obtained (block 0.75–1.0 × 0.5 cm), with bleeding controlled by direct pressure. The wound was closed with interrupted vicryl sutures.

Isolated focal limb perfusion. Methods are identical to those described in ref. 20, only rAAVrh74.MCK.GALGT2 was infused at a dose of 2×10^{12} vg/kg in 2.5 ml/kg of normal saline.

Immunosuppression and clinical monitoring. Immunosuppression regimens were identical to those described in ref. 20.

Assay of CT carbohydrate overexpression for GALGT2 transgene. All macaques treated by isolated limb perfusion were sacrificed at 12 or 24 weeks, at which time the entire gastrocnemius muscle was removed and blocked (0.75–1.0 × 0.5 cm blocks). Muscles were embedded in 7% gum tragacanth and flash frozen in isopentane cooled in liquid nitrogen. Cryostat sections (12 μm) were blocked for 1 hour in phosphate-buffered saline (PBS) with 3% bovine serum albumin, incubated overnight with anti-CT2 polyclonal primary antibody, as hybridoma supernatant diluted 1:2 in PBS with 3% bovine serum albumin at 4 °C, washed for 1 hour with PBS at 25 °C in a wet chamber, incubated with Cy2-conjugated goat antimice IgM specific secondary (Jackson ImmunoResearch, West Grove, PA) antibody for 1 hour at 25 °C, washed with PBS three times, dried, and mounted with Vectashield mounting medium (Vector Laboratories, Burlingame, CA). Fluorescence staining was visualized using a Zeiss Axioskop2 Plus Microscope, and images were captured with a Zeiss AxioCam MRC5 camera using a fluorescein isothiocyanate fluorescence filter. The number of fibers with sarcolemmal staining was expressed as percentage of all fibers. Means were obtained by counting four 10× fields from each muscle block (12–18 blocks per head of gastrocnemius).

qPCR of viral genomes. TaqMan qPCR was used to quantify the number of AAV vector genome copies in treated gastrocnemius muscle compared with contralateral control tissue and nontargeted organs, as previously described.[47,48] Ten to 25 mg of tissue was used to extract DNA. A vector-specific primer probe set (forward: 5′-CCTCAGTGGATGTTGCCTTTA, probe: 5′-FAM/AAAGCTGCG/ZEN/GAATTGTACCCGC/3IABkFQ, and reverse: 5′ATCTTGAGGAGCCACAGAAATC) amplified a portion of the MCK promoter just 5′ to the transgene along with the 5′-most region of the GALGT2 transgene by TaqMan RT-PCR, as before.[47,48] This primer set did not amplify endogenous *Macca mulatta GALGT2* gene sequence or endogenous MCK promoter elements. Along with assayed tissue samples, the plasmid used to make rAAVrh74.MCK.GALGT2 was linearized with ClaI and used to generate a standard curve from 5×10^1 to 5×10^6 copy number for each assay. Such standard curves had Pearson correlation coefficients of 0.98 or above and did not yield any signal without plasmid present. Copy number is reported as vector genomes per microgram of genomic DNA.

Enzyme-linked immunosorbent spot assay. Assays were performed as in ref. 20, only assays for GALGT2 utilized two pools of 20 amino acid peptides encompassing the entire human GALGT2 protein sequence.

Anti-rAAVrh74 antibody assay. Assays were done as described in ref. 20.

Quantification of Myofiber Diameter. Dissected segments of the gastrocnemius muscle were snap frozen in liquid nitrogen-cooled isopentane. Frozen muscle blocks from treated gastrocnemius muscles and the contralateral control muscles from the same macaques were cut in cross-section at 8–10 μm on a cryostat and stained with hematoxylin and eosin, as before.[1] Five to six representative 94,000 μm^2 images per block were captured on a Zeiss Axophot microscope and myofiber diameters (mini-Feret diameter) were measured using Zeiss AxioVision LE 4.1 imaging software, as before.[5,8] The average myofiber diameter was calculated from multiple images of six treated and six contralateral control muscle blocks.

Quantification of muscle fiber type. Dissected segments of the gastrocnemius muscle were snap frozen in liquid nitrogen-cooled isopentane. Frozen muscle blocks from treated gastrocnemius muscles and the contralateral control muscles from the same macaques were cut in cross-section at 8–10 μm on a cryostat and stained for Myosin ATPase activity at pH 4.3, as before.[1] For this method, type 1 (slow) fibers stain black, while type 2 (fast) fibers remain white.[49] Three representative 374,000 μm^2 area images per block were captured on a Zeiss Axiophot microscope using Zeiss AxioVision LE 4.1 imaging software. An average of 500–1,000 myofibers were counted per muscle section as either type I (black) or type II (white), with six treated and six contralateral muscle blocks counted from three different macaques per condition.

T-cell proliferation assay. Assays were done as described in ref. 20.

Immunostaining. Segments of gastrocnemius muscles from treated and untreated rhesus macaques were snap frozen in liquid nitrogen-cooled isopentane and sectioned at 8–10 μm on a cryostat. For immunostaining with carbohydrate-specific reagents (CT2 (made in our laboratory from the original hybridoma cells or WFA (EY laboratories, San Mateo, CA), sections were blocked in PBS with 1 mg/ml bovine serum albumin. For all other stains (CD8 (Abd Serotec, Oxford, UK), MCA1226F), CD14 (BD Pharmingen, San Jose, CA, 557153), CD16 (BioLegend, San Diego, CA, 302005), α dystroglycan (IIH6, Upstate Biotechnology, Lake Placid, NY), β dystroglycan (43DAG, Nova Castra (Leica), Buffalo Grove, IL) and MANDAG2, Developmental Studies Hybridoma bank (Iowa City, IA), dystrophin (Dys1, Nova Castra), utrophin (Drp1 and Drp2, Nova Castra), laminin α2 (gift from Ling Guo and Eva Engvall), laminin α5 (rabbit polyclonal, gift from Jeffery Miner), Plectin1 (10F6, Santa Cruz Biotechnology, Santa Cruz, CA), agrin (H-300, Santa Cruz Biotechnology), α sarcoglycan (Ad1, Nova Castra), β sarcoglycan (βSarc1, Nova Castra), γ sarcoglycan (35DAG2, Nova Castra), δ sarcoglycan (δSarc3, Nova Castra), sections were blocked in PBS with 10% goat serum. WFA and all CD antibodies were directly conjugated to fluorescein isothiocyanate. All other antibodies used were unlabeled and required use of a labeled secondary antibody for visualization. Primary antibodies were added overnight at 4 °C. Sections were washed in PBS, incubated with appropriate fluorophore-conjugated secondary antibody (all from Jackson ImmunoResearch), washed, dried, and mounted in glycerol containing paraphenylenediamine to inhibit fluorescence quenching. Neuromuscular junctions were visualized by costaining with 50 nmol/l rhodamine-α-bungarotoxin (Molecular Probes, Eugene, OR). Staining was visualized on a Zeiss

Axiophot epifluorescence microscope with appropriate rhodamine-or fluorescein-specific filters and using Zeiss AxioVision LE 4.1 imaging software. For comparisons of GALGT2-treated and untreated or contralateral treated muscles, all comparisons from each antibody stain were time-matched for exposure and the same concentration of antibody was used for staining.

Lectin precipitation. Gastrocnemius muscles were dissected, minced, and solubilized in Tris-buffered saline pH 7.4 1% Nonidet-P40 (NP-40) with shaking overnight at 4 °C. The concentration of extracted protein was determined by a modified Bradford assay, after which differing amounts of extracted proteins (3.0, 1.0, 0.5, or 0.15 mg) were precipitated with WFA or WGA conjugated to agarose at 4 °C overnight. Pellets were spun at 1,000*g* for 3 minutes, washed 2–3 times with lysis buffer, and precipitated material solubilized with sodium dodecyl sulfate buffer, separated by sodium dodecyl sulfate-polyacrylamide gel electrophoresis on 4–12% gradient gels, and immunoblotted to identify precipitated proteins, as described previously.[6]

Immunoblotting. Gastrocnemius muscles were dissected, minced, and solubilized in Tris-buffered saline pH 7.4 1% Nonidet-P40 (NP-40) with shaking overnight at 4 °C. The concentration of extracted protein was determined by a modified Bradford assay, after which protein was denatured by boiling in 1% sodium dodecyl sulfate with 1% β-mercaptoethanol. Ten to 40 μg per lane of whole-cell protein was separated by sodium dodecyl sulfate-polyacrylamide gel electrophoresis on 4–12% gradient gels and analyzed by semi-quantitative Western blotting, as previously described.[50] Antibodies listed for immunostaining were also used for immunoblotting. In addition, GALGT2 blots were probed with a polyclonal antiserum (NBP1-91229) from Novus Biologicals (Littleton, CO), and GAPDH immunoblots were probed with antibody MAB374 from Millipore (Billerica, MA).

Semi-qRT-PCR. Relative transcription levels were assessed by qRT-PCR by the delta-delta-CT method using GAPDH as an internal reference. Total RNA was isolated using Trizol reagent (Invitrogen (Life Technologies) Grand Island, NY) from gastrocnemius muscle blocks, where expression of GALGT2 had already been assessed by immunostaining and purified on a silica gel–based membrane (RNeasy, Qiagen, Germantown, MD). The integrity of RNA was verified by capillary electrophoresis using a 6000 Nano LabChip kit on a Bioanalyzer 2100 (Agilent, Santa Clara, CA). RNA content was measured using an ND-1000 spectrophotometer (Nano-drop). Only samples with no evidence of degradation were used. A high capacity cDNA archive kit (Applied Biosystems) was used to reverse transcribe RNA per manufacturer guidelines. Samples were subjected to RT-PCR in triplicate using a TaqMan ABI 7500 sequence detection system (Applied Biosystems) with GAPDH as internal reference. Primer sets were designed using PrimerQuest DNA software and synthesized by Integrated DNA Technologies (Coralville, IA) For data shown in Figure 8b, primers used were as follows: *Homo sapiens GALGT2*: GAA CGT CTC AGG AAC CTC TTT (forward), FAM/CG ATG GAA T/Zen/C TGG CTG TTC CCG AA/3IABkFQ (probe), GTT GTA ACC TCC CTG CTC TTT (reverse); *M. mulatta UTRN*: GGC AAC CAA CTG ATA ACA CAA G (forward), FAM/TC TGC TGA A/Zen/T GCT AGA TGG GAG GC/3IABkFQ (probe), GTC CAT ACT CTC CAC CCT AAG A (reverse), *M. mulatta DAG1:* AAT CCT GTT CTC TGT GGC TAT G (forward), FAM/TC TGC TGA A/Zen/T GCT AGA TGG GAG GC/3IABkFQ (probe), GTC CAT ACT CTC CAC CCT AAG A (reverse), *M. mulatta DMD*: GTC AGG GTC AAT TCT CTC ACT C (forward), FAM/TT GCT CTT C/Zen/C AAA GCA GCA GTT GC/3IABkFQ (probe), GCC CAT CGA TCT CCC AAT AC (reverse), *M. mulatta PLEC1*: GAT ATG ACG GCC AAG GAG AAG (forward), FAM/TG CGA TGT G/Zen/A CAA CTT CAC CTC CA/3IABkFQ (probe), TGG ATG ATG GCG TTG AAG AG (reverse), *M. mulatta LAMA2*: GTG GCA GAG TCC CAG TAT TAA G (forward), FAM/AC ACT GGA T/Zen/T TAC AGC AGG TGT TCC A/3IABkFQ (probe), CCT TCA CAA TCA CAT ACG CAA TC (reverse), *M. mulatta LAMA5*: CCT GGA GAA TGG AGA GAT TGT G (forward), FAM/AG CAG CGG C/Zen/G AGT AGG AGA AAT TC/3IABkFQ61 (probe), GTT AGT GGC CTT GGT GAA CT (reverse), *M. mulatta AGRN*: CGG TAC TTG AAG GGC AAA GA (forward), FAM/TGG TGA TCA /ZEN/ GCG GCT TTG GAG A/3IABkFQ (probe), ACA CCT GGT TGT CAC AGA TG (reverse), *M. mulatta GAPDH*: CCC TTC ATT GAC CTC AAC TAC A (forward), FAM/TG ATT CCA C/Zen/C CAT GGC AAG TTC CA/3IABkFQ (probe), and TCC ATT GAT GAC GAG CTT CC (reverse). For data shown in **Figure 3b**, primer sets were designed only to recognize *H. sapiens GALGT2* (CTACGATGGAATCTGGCTGTT (forward), 56-FAM/ATCCAACAA/Zen/AGAGCAGGGAGGTTA/3IABkFQ (probe), GCCATAGGCATCCTGAAAGT (reverse), *M. mulatta GAL GT2* (TGAGGAGACAGGCTGAATTTG (forward), 56-FAM/ACTTT CAGA/Zen/GGAGAGAAGGGCTGC/3IABkFQ (probe), or *M. mulatta GAPDH* (CCCTTCATTGACCTCAACTACA (forward), FAM/TGATT CCAC/Zen/CCATGGCAAGTTCCA/3IABkFQ (probe), TCCATTGATG ACGAGCTTCC (reverse). The protocol was repeated twice, once with all steps done as above and once with all steps done identically but for the elimination of reverse transcriptase from the RT step to determine and subtract background signal emanating from viral genomes present in the tissue.

SUPPLEMENTARY MATERIAL

Figure S1. Stratification scheme and experimental timeline.
Figure S2. Lack of change in fiber-type composition in GALGT2-treated muscles.
Figure S3. Evidence of mononuclear cell infiltrates in two rAAVrh74.MCK.GALGT2-treated subjects with positive IFN-γ ELISpot responses to human GALGT2 P5 peptide.
Figure S4. Altered expression of utrophin, plectin1, agrin, and laminin α5 protein in GALGT2-treated muscles.
Figure S5. Unchanged pattern of immunostaining for dystrophin, laminin α2, and β dystroglycan in GALGT2-treated muscles.
Figure S6. Anti-CT2 immunoblot of WFA and WGA lectin precipitations from 24-week GALGT2-treated macaque muscle.
Figure S7. Anti-β dystroglycan immunoblot of WFA and WGA lectin precipitations from 24-week GALGT2-treated macaque muscle.
Table S1. Clinical chemistries after rAAVrh74.MCK.GALGT2 treatment in rhesus macaques.

ACKNOWLEDGMENTS

We thank the Viral Vector Core at Nationwide Children's Hospital for vector production. This research was supported by the Children's Hospital Foundation (J.R.M.) and National Institutes of Health U54 NS055958 (J.R.M.) and R01 AR060949 (P.T.M.) and Jesse's Journey Foundation (L.R.R.K., L.G.C., and J.R.M.). The authors specially thank Jeffery Miner (Washington University) for laminin α5 antibody and Ling Guo and Eva Engvall (UC San Diego) for polyclonal antibody specific to laminin α2. The authors have nothing to disclose.

REFERENCES

1. Xia, B, Hoyte, K, Kammesheidt, A, Deerinck, T, Ellisman, M and Martin, PT (2002). Overexpression of the CT GalNAc transferase in skeletal muscle alters myofiber growth, neuromuscular structure, and laminin expression. *Dev Biol* **242**: 58–73.
2. Nguyen, HH, Jayasinha, V, Xia, B, Hoyte, K and Martin, PT (2002). Overexpression of the cytotoxic T cell GalNAc transferase in skeletal muscle inhibits muscular dystrophy in mdx mice. *Proc Natl Acad Sci USA* **99**: 5616–5621.
3. Martin, PT (2003). Glycobiology of the neuromuscular junction. *J Neurocytol* **32**: 915–929.
4. Martin, PT, Scott, LJ, Porter, BE and Sanes, JR (1999). Distinct structures and functions of related pre- and postsynaptic carbohydrates at the mammalian neuromuscular junction. *Mol Cell Neurosci* **13**: 105–118.
5. Xu, R, Camboni, M and Martin, PT (2007). Postnatal overexpression of the CT GalNAc transferase inhibits muscular dystrophy in mdx mice without altering muscle growth or neuromuscular development: evidence for a utrophin-independent mechanism. *Neuromuscul Disord* **17**: 209–220.
6. Yoon, JH, Chandrasekharan, K, Xu, R, Glass, M, Singhal, N and Martin, PT (2009). The synaptic CT carbohydrate modulates binding and expression of extracellular

matrix proteins in skeletal muscle: partial dependence on utrophin. *Mol Cell Neurosci* **41**: 448–463.
7. Martin, PT, Xu, R, Rodino-Klapac, LR, Oglesbay, E, Camboni, M, Montgomery, CL *et al.* (2009). Overexpression of Galgt2 in skeletal muscle prevents injury resulting from eccentric contractions in both mdx and wild-type mice. *Am J Physiol, Cell Physiol* **296**: C476–C488.
8. Xu, R, Chandrasekharan, K, Yoon, JH, Camboni, M and Martin, PT (2007). Overexpression of the cytotoxic T cell (CT) carbohydrate inhibits muscular dystrophy in the dyW mouse model of congenital muscular dystrophy 1A. *Am J Pathol* **171**: 181–199.
9. Xu, R, DeVries, S, Camboni, M and Martin, PT (2009). Overexpression of Galgt2 reduces dystrophic pathology in the skeletal muscles of alpha sarcoglycan-deficient mice. *Am J Pathol* **175**: 235–247.
10. Tinsley, J, Deconinck, N, Fisher, R, Kahn, D, Phelps, S, Gillis, JM *et al.* (1998). Expression of full-length utrophin prevents muscular dystrophy in mdx mice. *Nat Med* **4**: 1441–1444.
11. Burkin, DJ, Wallace, GQ, Nicol, KJ, Kaufman, DJ and Kaufman, SJ (2001). Enhanced expression of the alpha 7 beta 1 integrin reduces muscular dystrophy and restores viability in dystrophic mice. *J Cell Biol* **152**: 1207–1218.
12. Peter, AK, Marshall, JL and Crosbie, RH (2008). Sarcospan reduces dystrophic pathology: stabilization of the utrophin-glycoprotein complex. *J Cell Biol* **183**: 419–427.
13. Gawlik, K, Miyagoe-Suzuki, Y, Ekblom, P, Takeda, S and Durbeej, M (2004). Laminin alpha1 chain reduces muscular dystrophy in laminin alpha2 chain deficient mice. *Hum Mol Genet* **13**: 1775–1784.
14. Bentzinger, CF, Barzaghi, P, Lin, S and Ruegg, MA (2005). Overexpression of mini-agrin in skeletal muscle increases muscle integrity and regenerative capacity in laminin-alpha2-deficient mice. *FASEB J* **19**: 934–942.
15. Rodino-Klapac, LR, Janssen, PM, Montgomery, CL, Coley, BD, Chicoine, LG, Clark, KR *et al.* (2007). A translational approach for limb vascular delivery of the micro-dystrophin gene without high volume or high pressure for treatment of Duchenne muscular dystrophy. *J Transl Med* ***5***: 45.
16. Wang, Z, Zhu, T, Qiao, C, Zhou, L, Wang, B, Zhang, J *et al.* (2005). Adeno-associated virus serotype 8 efficiently delivers genes to muscle and heart. *Nat Biotechnol* **23**: 321–328.
17. Gao, GP, Alvira, MR, Wang, L, Calcedo, R, Johnston, J and Wilson, JM (2002). Novel adeno-associated viruses from rhesus monkeys as vectors for human gene therapy. *Proc Natl Acad Sci USA* ***99***: 11854–11859.
18. Rapti, K, Louis-Jeune, V, Kohlbrenner, E, Ishikawa, K, Ladage, D, Zolotukhin, S *et al.* (2012). Neutralizing antibodies against AAV serotypes 1, 2, 6, and 9 in sera of commonly used animal models. *Mol Ther* **20**: 73–83.
19. Hoyte, K, Kang, C and Martin, PT (2002). Definition of pre- and postsynaptic forms of the CT carbohydrate antigen at the neuromuscular junction: ubiquitous expression of the CT antigens and the CT GalNAc transferase in mouse tissues. *Brain Res Mol Brain Res* **109**: 146–160.
20. Chicoine, LG, Montgomery, CL, Bremer, WG, Shontz, KM, Griffin, DA, Heller, KN *et al.* (2013). Plasmapheresis eliminates the negative Impact of AAV antibodies on microdystrophin gene expression following vascular delivery. *Mol Ther* advance online publication 3 December 2013; doi:10.1038/mt.2013.244.
21. Mendell, JR, Moxley, RT, Griggs, RC, Brooke, MH, Fenichel, GM, Miller, JP *et al.* (1989). Randomized, double-blind six-month trial of prednisone in Duchenne's muscular dystrophy. *N Engl J Med* **320**: 1592–1597.
22. Mingozzi, F and High, KA (2011). Therapeutic *in vivo* gene transfer for genetic disease using AAV: progress and challenges. *Nat Rev Genet* **12**: 341–355.
23. Montiel, MD, Krzewinski-Recchi, MA, Delannoy, P and Harduin-Lepers, A (2003). Molecular cloning, gene organization and expression of the human UDP-GalNAc:Neu5Acalpha2-3Galbeta-R beta1,4-N-acetylgalactosaminyltransferase responsible for the biosynthesis of the blood group Sda/Cad antigen: evidence for an unusual extended cytoplasmic domain. *Biochem J* **373**(Pt 2): 369–379.
24. Meier, T, Marangi, PA, Moll, J, Hauser, DM, Brenner, HR and Ruegg, MA (1998). A minigene of neural agrin encoding the laminin-binding and acetylcholine receptor-aggregating domains is sufficient to induce postsynaptic differentiation in muscle fibres. *Eur J Neurosci* **10**: 3141–3152.
25. Martin, LT, Glass, M, Dosunmu, E and Martin, PT (2007). Altered expression of natively glycosylated alpha dystroglycan in pediatric solid tumors. *Hum Pathol* **38**: 1657–1668.
26. Yoon, JH, Johnson, E, Xu, R, Martin, LT, Martin, PT and Montanaro, F (2012). Comparative proteomic profiling of dystroglycan-associated proteins in wild type, mdx, and Galgt2 transgenic mouse skeletal muscle. *J Proteome Res* **11**: 4413–4424.
27. Rezniczek, GA, Konieczny, P, Nikolic, B, Reipert, S, Schneller, D, Abrahamsberg, C *et al.* (2007). Plectin 1f scaffolding at the sarcolemma of dystrophic (mdx) muscle fibers through multiple interactions with beta-dystroglycan. *J Cell Biol* **176**: 965–977.
28. Rafael, JA, Tinsley, JM, Potter, AC, Deconinck, AE and Davies, KE (1998). Skeletal muscle-specific expression of a utrophin transgene rescues utrophin-dystrophin deficient mice. *Nat Genet* **19**: 79–82.
29. Ehrig, K, Leivo, I, Argraves, WS, Ruoslahti, E and Engvall, E (1990). Merosin, a tissue-specific basement membrane protein, is a laminin-like protein. *Proc Natl Acad Sci USA* **87**: 3264–3268.
30. Manno, CS, Pierce, GF, Arruda, VR, Glader, B, Ragni, M, Rasko, JJ *et al.* (2006). Successful transduction of liver in hemophilia by AAV-Factor IX and limitations imposed by the host immune response. *Nat Med* **12**: 342–347.
31. Mingozzi, F and High, KA (2013). Immune responses to AAV vectors: overcoming barriers to successful gene therapy. *Blood* **122**: 23–36.
32. Kornegay, JN, Bogan, JR, Bogan, DJ, Childers, MK, Li, J, Nghiem, P *et al.* (2012). Canine models of Duchenne muscular dystrophy and their use in therapeutic strategies. *Mamm Genome* **23**: 85–108.
33. Murphy, SL, Li, H, Zhou, S, Schlachterman, A, High, KA and High, K (2008). Prolonged susceptibility to antibody-mediated neutralization for adeno-associated vectors targeted to the liver. *Mol Ther* **16**: 138–145.
34. Jiang, H, Couto, LB, Patarroyo-White, S, Liu, T, Nagy, D, Vargas, JA *et al.* (2006). Effects of transient immunosuppression on adenoassociated, virus-mediated, liver-directed gene transfer in rhesus macaques and implications for human gene therapy. *Blood* **108**: 3321–3328.
35. Monteilhet, V, Saheb, S, Boutin, S, Leborgne, C, Veron, P, Montus, MF *et al.* (2011). A 10 patient case report on the impact of plasmapheresis upon neutralizing factors against adeno-associated virus (AAV) types 1, 2, 6, and 8. *Mol Ther* **19**: 2084–2091.
36. Sack, BK, Merchant, S, Markusic, DM, Nathwani, AC, Davidoff, AM, Byrne, BJ *et al.* (2012). Transient B cell depletion or improved transgene expression by codon optimization promote tolerance to factor VIII in gene therapy. *PLoS ONE* **7**: e37671.
37. Mingozzi, F, Chen, Y, Edmonson, SC, Zhou, S, Thurlings, RM, Tak, PP *et al.* (2013). Prevalence and pharmacological modulation of humoral immunity to AAV vectors in gene transfer to synovial tissue. *Gene Ther* **20**: 417–424.
38. Mendell, JR, Campbell, K, Rodino-Klapac, L, Sahenk, Z, Shilling, C, Lewis, S *et al.* (2010). Dystrophin immunity in Duchenne's muscular dystrophy. *N Engl J Med* **363**: 1429–1437.
39. Dohi, T, Yuyama, Y, Natori, Y, Smith, PL, Lowe, JB and Oshima, M (1996). Detection of N-acetylgalactosaminyltransferase mRNA which determines expression of Sda blood group carbohydrate structure in human gastrointestinal mucosa and cancer. *Int J Cancer* ***67***: 626–631.
40. Dohi, T and Kawamura, YI (2008). Incomplete synthesis of the Sda/Cad blood group carbohydrate in gastrointestinal cancer. *Biochim Biophys Acta* **1780**: 467–471.
41. Morton, JA, Pickles, MM and Terry, AM (1970). The Sda blood group antigen in tissues and body fluids. *Vox Sang* **19**: 472–482.
42. Tinsley, JM, Fairclough, RJ, Storer, R, Wilkes, FJ, Potter, AC, Squire, SE *et al.* (2011). Daily treatment with SMTC1100, a novel small molecule utrophin upregulator, dramatically reduces the dystrophic symptoms in the mdx mouse. *PLoS ONE* ***6***: e19189.
43. Gao, G, Lebherz, C, Weiner, DJ, Grant, R, Calcedo, R, McCullough, B *et al.* (2004). Erythropoietin gene therapy leads to autoimmune anemia in macaques. *Blood* **103**: 3300–3302.
44. Chenuaud, P, Larcher, T, Rabinowitz, JE, Provost, N, Cherel, Y, Casadevall, N *et al.* (2004). Autoimmune anemia in macaques following erythropoietin gene therapy. *Blood* **103**: 3303–3304.
45. Marshall, JL, Holmberg, J, Chou, E, Ocampo, AC, Oh, J, Lee, J *et al.* (2012). Sarcospan-dependent Akt activation is required for utrophin expression and muscle regeneration. *J Cell Biol* **197**: 1009–1027.
46. Rabinowitz, JE, Rolling, F, Li, C, Conrath, H, Xiao, W, Xiao, X *et al.* (2002). Cross-packaging of a single adeno-associated virus (AAV) type 2 vector genome into multiple AAV serotypes enables transduction with broad specificity. *J Virol* **76**: 791–801.
47. Clark, KR, Liu, X, McGrath, JP and Johnson, PR (1999). Highly purified recombinant adeno-associated virus vectors are biologically active and free of detectable helper and wild-type viruses. *Hum Gene Ther* **10**: 1031–1039.
48. Rodino-Klapac, LR, Montgomery, CL, Bremer, WG, Shontz, KM, Malik, V, Davis, N *et al.* (2010). Persistent expression of FLAG-tagged micro dystrophin in nonhuman primates following intramuscular and vascular delivery. *Mol Ther* **18**: 109–117.
49. Hämäläinen, N and Pette, D (1993). The histochemical profiles of fast fiber types IIB, IID, and IIA in skeletal muscles of mouse, rat, and rabbit. *J Histochem Cytochem* **41**: 733–743.
50. Hoyte, K, Jayasinha, V, Xia, B and Martin, PT (2004). Transgenic overexpression of dystroglycan does not inhibit muscular dystrophy in mdx mice. *Am J Pathol* **164**: 711–718.